Investigation of the ternary phase diagram of Au–Pb–Rh compounds

Nikola Subotić[1], Takashi Mochiku[2], Yoshitaka Matsushita[2], Mitsuaki Nishio[2], Osamu Takeuchi[1], Hidemi Shigekawa[1], Kazuo Kadowaki[1]

[1]University of Tsukuba, 1-1-1 Tenoudai, Tsukuba, Ibaraki 305-8573, Japan
[2]National Institute for Material Science, 1-2-1 Sengen, Tsukuba, Ibaraki 305-0047, Japan

Abstract

The ternary phase diagram of the Pb-rich Au–Pb–Rh system has been studied from a viewpoint of the formation of intermetallic compounds. We indeed discovered two new compounds with the nominal chemical formula of $AuPb_2Rh_2$ and $AuPb_4Rh_5$. They are revealed by XRD study to possess a similar crystal structure with each other having an orthorhombic crystal structure with *Pmma* symmetry. The resistivity measurements of $AuPb_2Rh_2$ show double superconducting transitions at 2.8 K and 1.7 K, while $AuPb_4Rh_5$ did not above 1.1 K. The significant shift of stoichiometric ratio of Au and Rh observed in both compounds suggests strongly that vacancy structures and site exchange, in particular, the $AuPb_4Rh_5$ compound, may play an important role in the physical properties of these compounds.

Introduction

Recently, the topological nature of the electronic state of matter has attracted much theoretical as well as experimental attention, because it has emerged newly as a quantum state of matter in solid-state physics [1–4]. Materials that possess such behavior, for example, resistanceless surface current, may be expected as the most valuable for practical application. According to the band calculations, so far, many materials have been listed and nominated as candidate materials [5–7]. For this purpose of the study, we have chosen the ternary intermetallic compounds including Pb and 4d or 5d transition metal elements as the main work field because Pb is the heaviest stable element, nonradioactive, easy to handle, forming stable compounds with 4d and 5d elements, with large spin-orbital interaction, a common cheap metal, etc.

The binary phase diagram Pb-Rh has been investigated [8, 9]. According to [8] the stable intermediate compounds are $RhPb_4$, $RhPb_2$, Rh_4Pb_5, RhPb, and Rh_3Pb_2. Besides the before-mentioned compounds, according to [9], Rh_5Pb_7 and Rh_3Pb are stable. The superconducting properties of $RhPb_2$ might be influenced by Rh deficiency [10, 11]. RhPb belongs to the CoSn-type structure, exhibiting a flat electronic band that could induce unconventional superconductivity, magnetism, and topological behaviors [12]. Rh_4Pb_5 might also exhibit topological properties since its topological Z_2 index is (0;1,0,1) [13], while, according to [14],

Rh_4Pb_5 is a topo- logical crystalline insulator.

Compared to the binary phase diagram Pb–Rh, the binary phase diagram Au–Pb is simpler. According to [15], the following intermediate states are stable: $AuPb_2$, Au_2Pb, and $AuPb_3$ while one metastable state Au_2Pb_3 has been reported. Among them, Au_2Pb is a topological superconductor candidate [16] having three different phases at a lower temperature, while the Z_2 index related to the $AuPb_3$ compound is (1;1,1,1) [13]. It is interesting to note that similar controversy exists regarding the superconducting transition temperatures of $AuPb_2$ and $AuPb_3$ as in the $RhPb_2$ case. The binary phase diagram Au-Rh has no stable intermediate compounds.

Considering the above-mentioned binary systems for Pb–Rh and Au–Pb, we started to look for compounds from higher concentrations of Pb in the ternary system, because Pb is expected to promote intermediate compounds to form a flux, which may also interact as a component of the inter- metallic compounds.

Materials and methods

The examined molar ratios were as follows: 1:4:1 = Au:Pb:Rh, 3:5:1 = Au:Pb:Rh, 2:8:1 = Au:Pb:Rh, 2:2:1 = Au:Pb:Rh. The raw materials of Au and Pb were 99.9% purity in shots while Rh was 99.9% purity in pow- der form (300 mesh), purchased from Furuuchi Chemical Co, Japan. Before the crystal growth, the corresponding amount of the material was heated gently and melted in an evacuated quartz tube by the flame torch. The melted ingot was put in another evacuated quartz tube and heat-treated with the following temperature profile in a standard muffle furnace; 900°C for one day, decreasing to 800°C with a constant rate of 5 °C/h and then decreasing to 650°C with a constant rate of 1 °C/h.

After opening all the quartz tubes, the grown boules were spalled for further investigation. It was interesting to see many shiny crystals on the surface of the broken boules in all cases we studied. These crystals were extracted from the piece of the fragment and used for EPMA, XRD, and resistivity measurements. The standard four-point contact method was applied to measure the temperature dependence of resistivity. The silver paste was used to connect the volt- age and current leads. The contact resistance was typically below 1 Ω. The EPMA measurements were performed with JEOL JXA-8500F. The voltage and probe current were at 15 kV and 5 nA, respectively. For calibration, PbS, Au, and Rh were used. The XRD measurements were conducted with two circle diffractometer Rigaku Xtal Mini II.

Results

The many pieces of crystals were separated mostly by mechanical force, but in some cases, crystals can be found in the derbies of the sample. Although they are small (≤ 1 mm^3), they

can be used for the EPMA, XRD, and resistivity measurements.

The EPMA results are shown in Table 1. It is interesting to see that almost all crystals showed a high concentration of Rh even though the initial amount was the smallest. The COMPO images of the samples can also be found in the SI. For the 281 sample, only one measurement spot was chosen (results will be confirmed in near future). Crystals from the 141 sample might be assigned to $AuPb_4Rh_5$ while the 351 sample to $AuPb_2Rh_2$.

The single crystal XRD analysis has been performed for the two crystals as mentioned in Table 1. They were the crystals grown from 141 and 351 compositions (same as shown in Fig. 1a) and b)). The results were presented in Fig. 2. It is interesting to note that both crystals belong to the orthorhombic system with the same *Pmma* space group and the chemical formula can be identified to be $AuPb_2Rh_2$ and $AuPb_4Rh_5$. As seen from the crystal structures, the *b* lattice parameter of $AuPb_4Rh_5$ is almost double compared with that of $AuPb_2Rh_2$, indicating the formation of ordered vacancies structure and exchange of atomic positions along the *b*-axis by forming twinning pair of the basic unit cell of $AuPb_2Rh_2$. As a result, it seems that the structure of $AuPb_4Rh_5$ can adopt more site exchange of Au and Rh atoms in the middle of the unit cell in $AuPb_4Rh_5$.

This may also be supported by the evidence that the chemical stoichiometry of $AuPb_2Rh_2$ is naturally shifted from 1:4:5. Furthermore, it is found that the Rh atoms are slightly deficient as pointed out in previous work on $RhPb_2$ [10, 11]. A more detailed crystal structure analysis will be found elsewhere [17].

In Fig. 3 the temperature dependence of resistivity on samples 351 and 141 is shown. The resistivity at room temperature of the 141 sample is 640 $\mu\Omega$ cm while for the 351 sample is 81.6 $\mu\Omega$ cm. The residual resistance for both samples is high (around 480 $\mu\Omega$ cm for 141 sample and around 65 $\mu\Omega$ cm for 351). The corresponding RRR for 141 and 351 samples is 1.33 and 1.25, respectively. The 141 sample did not exhibit superconductivity down to 1.1 K while 351 had two transitions (2.8 K and 1.73 K). The ΔT_c for the 1.73 K transition is 0.17 K while for the 2.8 K transition is 1.2 K. The corresponding $\Delta T_c/T_c$ ratios are 0.098 and 0.42, respectively. The resistivity dependence on the temperature at higher temperatures is nearly linear. For 351 sample, the higher temperature part of the resistance is shown in SI where around 42 K, a slight kink can be observed.

Discussion and conclusion

The Pb-rich part of the Au-Pb-Rh ternary phase diagram has been investigated for the first time. Evidently, it becomes much more complicated; however, we have much more chances to find new compounds as expected. Indeed, we have so far discovered that two new compounds $AuPb_2Rh_2$ and $AuPb_4Rh_5$ can form in the Pb-rich ternary Au–Pb–Rh system.

In most cases, the grown crystals were rich in Rh even though the initial composition did not have such an amount of Rh. The highest concentration of Au in the measured crystals was not higher than 20% even though there were some cases where the initial concentration of Au was higher. This suggests that during the crystal growth phase separation might occur. In future, the phase diagram near the nominal concentration and narrower temperature range will be explored. In such conditions, the crystal quality should be improved by reducing the observed deficiency. Also, annealing the grown crystals at various temperatures will probably yield interesting results as well.

According to EPMA results, the crystals that were grown from the initial molar ratio of. 2:1:2 = Au:Rh:Pb and 1:1:4 = Au:Rh:Pb had similar compositions indicating that the $AuPb_4Rh_5$ forms at higher temperatures (around 850°C). At lower temperatures, the current situation is not clear, but the resistivity measurements indicate that other com- pounds are forming. Therefore, it is possible that at lower temperatures, other compounds form for the molar ratio of 2:2:1 = Au:Pb:Rh since those crystals are forming differently compared to the 1:4:1 = Au:Pb:Rh case (the crystals have formed on the surface opposite to the needle-like crystals forming inside the bulk). Moreover, the crystals that were grown from the 2:8:1 = Au:Pb:Rh ratio are interesting since the small concentration of Au suggests that doping of $RhPb_3$ occurred but according to [8, 9], $RhPb_3$ does not exist or doping of Rh-deficient $RhPb_2$ occurred. The Au-Rh-rich part of the phase diagram was not investigated, but it is expected that other compounds may form.

As for the superconductivity, uncertainty on the T_c still remains. This tendency is also similar in the binary systems of Au–Pb and Rh–Pb. $RhPb_2$ and related Rh-deficient structures have T_c = 1.26 K and 2.3 K, respectively [10], while Au_2Pb 1.18 K [16]. The situation regarding $AuPb_3$ and $AuPb_2$ is similar to $RhPb_2$ since the reported T_c values of those compounds do not agree with each other [18–20]. According to [19], the T_c of $AuPb_2$ is 4.42 K. On the other hand, [18] indicates that the 4.42 K transition is due to $AuPb_3$ while $AuPb_2$ becomes superconducting below 3.15 K. Surprisingly, $AuPb_4Rh_5$ is not superconducting above 1.1 K. For the $AuPb_2Rh_2$, its superconducting transition might be 1.7 K or 2.8 K. Although the main frame of the unit cell structure of $AuPb_2Rh_2$ and $AuPb_4Rh_5$ is very similar as seen in Fig. 2, the superconductivity transition behavior is very different. Therefore, one may ask how the T_c of these compounds is influenced by the Rh and Au deficiency and occupancy. Similar behavior was observed for $RhPb_2$ [10].

One may think a possibility that $AuPb_4Rh_5$ and $AuPb_2Rh_2$ can be derived from Rh_3Pb_2 doped with Au. However, this is unlikely since the crystal structure of Rh_3Pb_2 is hexagonal [8, 9]. Furthermore, there is a possibility that the binary phase diagram Rh–Pb may lack some crucial information because of its incompleteness [8, 9]. Certainly, we need more careful study in the

ternary Au–Pb–Rh system.

As mentioned in the introduction, some compounds from the binary phase diagrams Au–Pb and Rh–Pb are supposed to have nontrivial topological properties. For the ternary Au–Pb–Rh system, this situation may be similar. Two new compounds found in this study can also be such candidates for nontrivial topological materials. For example, the binary Au_2Pb system has intensively been studied as a possible non- trivial topological surface state [16, 21–24]. It is suggested to investigate theoretically and experimentally these new compounds. This was another motivation to discover new compounds.

In conclusion, the preliminary investigation of the ternary phase diagram Au–Pb–Rh has been performed and succeeded in discovering two new compounds $AuPb_4Rh_5$ and $AuPb_2Rh_2$. According to the XRD results, they belong to the orthorhombic crystal system (space group *Pmma*). $AuPb_4Rh_5$ is not superconducting above 1.1 K. The observed transition at 1.7 K and 2.8 K might be due to the different Rh deficiency and Au occupancy of $AuPb_2Rh_2$. In this sense, it is so curious to ask how nonstoichiometry, caused mainly by vacancies, affects the occurrence of superconductivity. To reveal such an interesting issue, the annealing study of the crystals under various conditions might be crucially important.

Acknowledgments

The author would like to thank Takanari Kashiwagi for the valuable discussion and support.

Data availability

The data that support the above-presented results are available from the corresponding author upon reasonable request.

Declarations

Conflict of interest

On behalf of all authors, the corresponding author states that there is no conflict of interest.

References

1. M.Z. Hasan, C.L. Kane, Rev. Mod. Phys. **82**, 3045 (2010)
2. K.V. Klitzing, G. Dorda, M. Pepper, Phys. Rev. Lett. **45**, 494 (1980)
3. C.L. Kane, E.J. Mele, Phys. Rev. Lett. **95**, 226801 (2005) 4. L. Fu, C.L. Kane, Phys. Rev. Lett. **100**, 096407 (2008)
5. M.G. Vergniory et al., Nature **566**, 480–485 (2019)
6. B. Bradlyn et al., Nature **547**, 298–305 (2017)
7. M.G. Vergniory et al., Science **376**, 9094 (2022)

8. B. Predel, Pb-Rh (Lead-Rhodium), in *Ni-Np–Pt-Zr* (1998), pp 1–2 9. G.R. Watts, *Gmelin Handbook of Inorganic and Organometallic*
Chemistry, System Number 64 Rh Rhodium, Supplement Volume A1: Coordination Compounds with O-and N-containing Ligands (Springer, Berlin, 1991)
10. N. Subotić et al., MRS Adv. **7**, 778 (2022)
11. T. Mochiku et al., Acta Crystallogr. Sect. E: Crystallogr. Com-
mun. **77**, 12 (2021)
12. W.R. Meier et al., Phys. Rev. B **102**, 075148 (2020)
13. Q.S. Wu, G. Autès, N. Mounet, O.V. Yazyev, Mater. Cloud Arch.
(2019). https://doi.org/10.24435/materialscloud:2019.0019/v1 14. T. Zhang et al., Nature **566**, 455 (2019)
15. H. Okamoto, T.B. Massalski, Bull. Alloy Phase Diag. **5**, 276–284
(1984)
16. L.M. Shoop et al., Phys. Rev. B **91**, 214517 (2015)
17. T. Mochiku et al., To be published in Acta Crystallogr. Sect. E 18. H.L. Caswell, Solid State Commun. **2**, 323–324 (1964)
19. M.F. Gendor, R.E. Jones, *J. Phys. Chem. Solids* **23**, 405–406
(1962)
20. J.P. Jan, A. Wegner, J. Low Temp. Phys. **13**, 195–208 (1973) 21. M.-V. Francisco et al., Phys. Rev. Res. **4**, 023241 (2022)
22. Y. Wu et al., Phys. Rev. B **98**, 161107 (2018)
23. Y. Xing et al., Nat. Quantum Mater. **1**, 16005 (2016)
24. K.W. Chen et al., Phys. Rev. B **93**, 045118 (2016)

Table 1 EPMA results for the crystals extracted from the grown boule with corresponding ratios of starting materials

Initial molar ratio	Au (%)	Pb (%)	Rh (%)
1:4:1 = Au:Pb:Rh	11.7	42.6	45.7
1:4:1 = Au:Pb:Rh	0.5	60.6	38.9
3:5:1 = Au:Pb:Rh	15	42.5	42.5
3:5:1 = Au:Pb:Rh	18.1	43.5	38.4
2:2:1 = Au:Pb:Rh	10.1	41.4	48.5
2:8:1 = Au:Pb:Rh	4.6	71.4	24

In the table, the averaged values are shown. The more detailed data are shown in SI

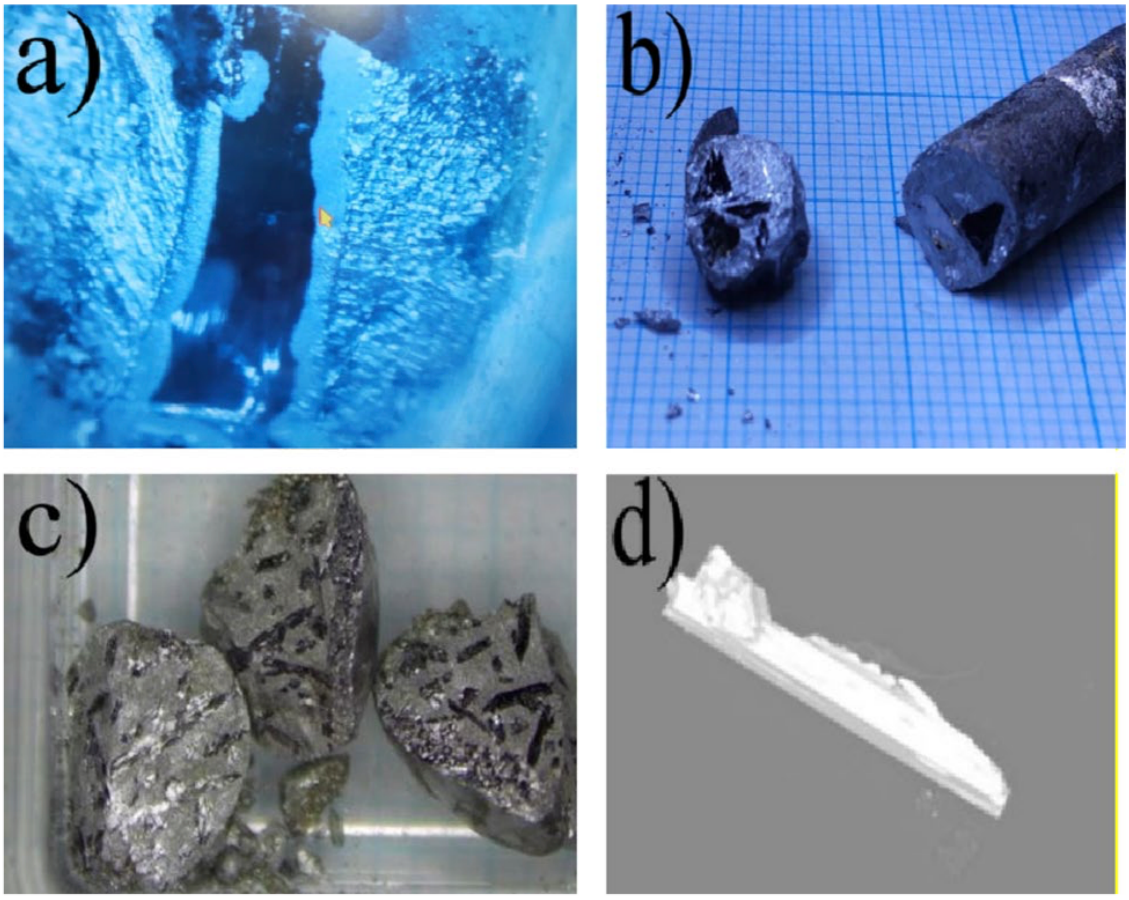

Fig. 1 **a** An optical photograph of the grown crystal from the start- ing composition of 1:4:1=Au:Pb:Rh. The crystal grows at the sur- face of the boule, whereas no crystal is found inside the boule. The size of the crystal is approximately as large as 12×4×2 mm3. **b** An optical photograph of the spalled boule with the initial composition of 3:5:1=Au:Pb:Rh. Large triangular plate-like crystals of more than a few millimeters in size were found inside the boule. The crystals seem to be cleavable because the same-sized crystal appears on both surfaces of the crushed boule almost every time. **c** An optical pho- tograph of the spalled boule grown from the starting composition of 2:2:1=Au:Pb:Rh. Many needle-like crystals can be seen inside the boule. The length of the needle can be as large as~5 mm with a width of~1 mm in diameter. **d** A COMPO image of the needle-like crystal extracted from the separated crystal grown from the starting composition of 2:8:1 = Au:Pb:Rh

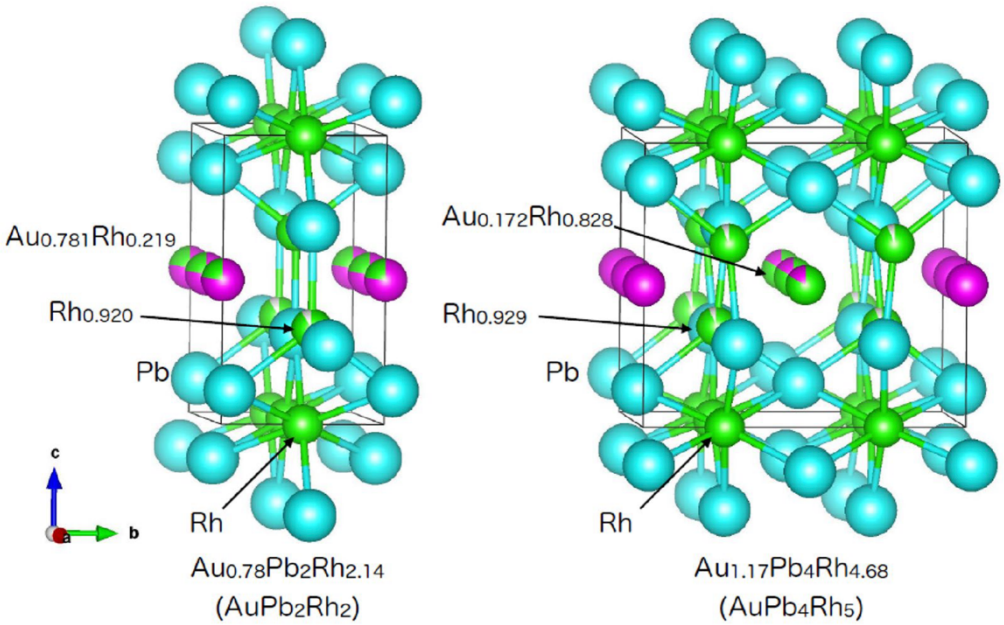

Crystal data	
Chemical formula	$Au_{0.78}Pb_2Rh_{2.14}$
M_r	788.24
Crystal system, space group	Orthorhombic, *Pmma*
Temperature (K)	297
a, *b*, *c* (Å)	5.6571 (4), 4.3335 (3), 7.6393 (5)
V (Å^3)	187.28 (2)
Z	2
Radiation type	Mo *Kα*
μ (mm^{-1})	128.57
Crystal size (mm)	0.06 × 0.02 × 0.01
R_{int}	0.042
Refinement	
$R[F^2 > 2\sigma(F^2)]$, $wR(F^2)$, S	0.016, 0.031, 1.15
No. of reflections	289
No. of parameters	24
$\Delta\rho_{max}$, $\Delta\rho_{min}$ (e Å^{-3})	1.73, −1.54

Crystal data	
Chemical formula	$Au_{1.17}Pb_4Rh_{4.68}$
M_r	1541.34
Crystal system, space group	Orthorhombic, *Pmma*
Temperature (K)	297
a, *b*, *c* (Å)	5.6473 (3), 8.6613 (4), 7.5922 (4)
V (Å^3)	371.36 (3)
Z	2
Radiation type	Mo *Kα*
μ (mm^{-1})	123.33
Crystal size (mm)	0.05 × 0.03 × 0.02
R_{int}	0.033
Refinement	
$R[F^2 > 2\sigma(F^2)]$, $wR(F^2)$, S	0.020, 0.044, 1.12
No. of reflections	554
No. of parameters	36
$\Delta\rho_{max}$, $\Delta\rho_{min}$ (e Å^{-3})	3.58, −2.23

Fig. 2 The results of XRD analysis of crystals 141 and 351. After careful refinement, the chemical compositions AuPb4Rh5 (141) and AuPb2Rh2 (351) were determined. The schematic atomic arrange- ments of the unit cell are shown. The Pb atoms are marked in blue, Rh in green, and Au in pink color. Crystal structures are quite similar (same space group) with different b lattice constants (about 2 times larger) and the total occupancy of the Au site for the AuPb4Rh5 is 1. Rh deficiency can be also observed in both cases which are not sub- stituted by Au atoms, similar to RhPb2 [10, 11]

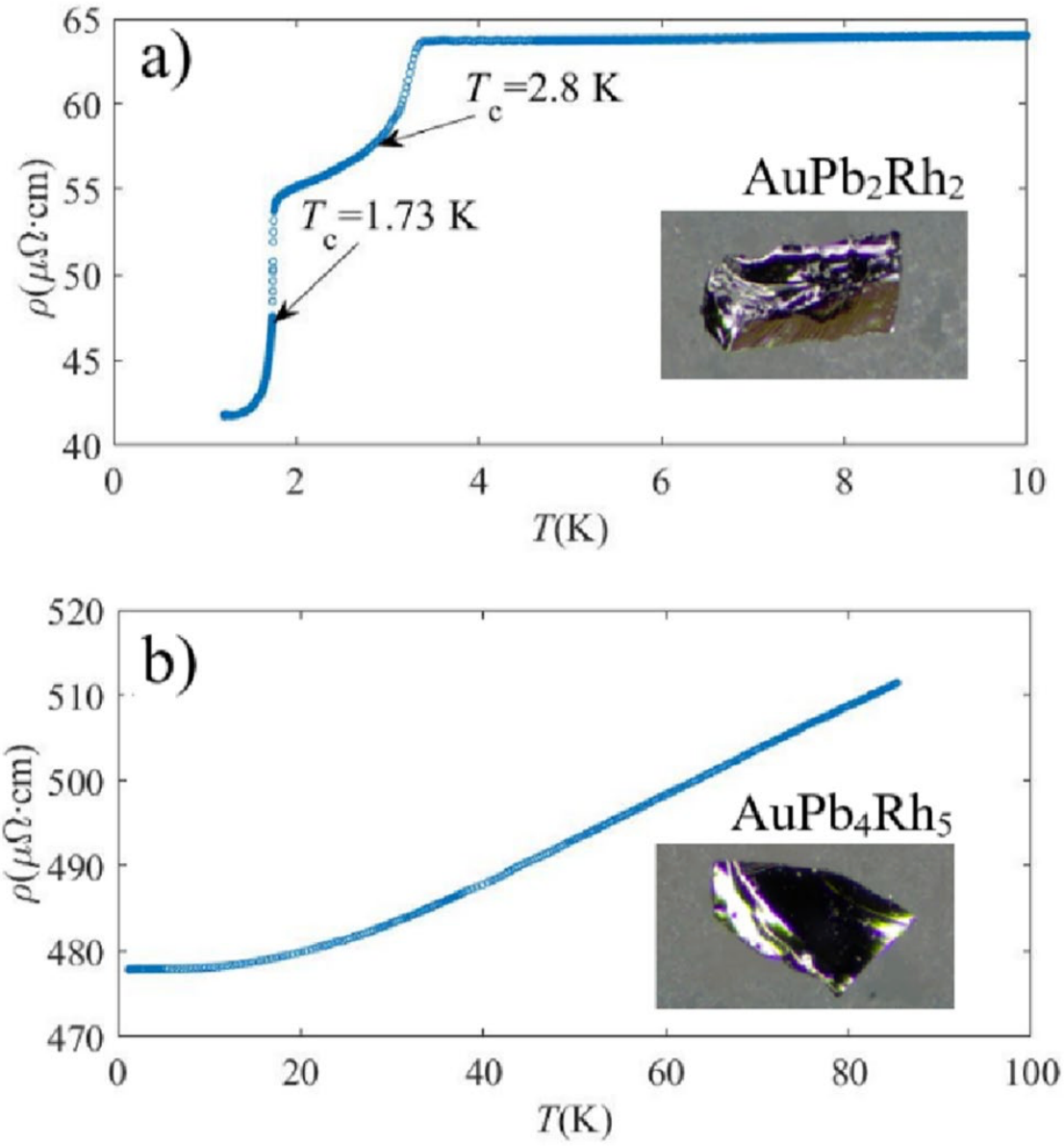

Fig. 3 a The low-temperature part of the resistivity plot of sample 351. The residual resistance is around 65 μ Ω cm while the room tem- perature resistivity is 81.6 μ Ω cm. The photograph of the measured crystal is shown in the inset. The resistivity plot up to 100 K is shown in the SI. The transition width of the 2.8 K transition (1.2 K) is wider than the 1.73 K transition (0.12 K). **b** Resistivity plot of 141 sam- ple up to 100 K. The sample did not exhibit superconductivity above 1.1 K. The linear dependence indicates the metallic behavior of 141 sample. The photograph of the measured crystal is shown in the inset